Neuroendocrinology Letters Volume 46 No. 7 2025
ISSN: 0172-780X; ISSN-L: 0172-780X; Electronic/Online ISSN: 2354-4716
Web of Knowledge / Web of Science: Neuroendocrinol Lett
Pub Med / Medline: Neuro Endocrinol Lett

ORIGINAL ARTICLE

Analysis of Mutation Site Structure Prediction and Family Characteristics of Maturity-Onset Diabetes of the Young (MODY) with Ketosis: Caused by HNF4α Gene Mutation

Jie Lu[1*], Jilai Zhang[2*], Xianling Wang[2]

1 Department of Endocrinology and Metabolism, Guangxi Academy of Medical Sciences and the People's Hospital of Guangxi Zhuang Region, Nanning, China.
2 Department of Endocrinology, The First Medical Center of PLA General Hospital, Beijing, China.

*Jie Lu and Jilai Zhang contributed equally to this article.

Correspondence to: Xianling Wang
Department of Endocrinology, The First Medical Center of Chinese PLA General Hospital, No.28 Fuxing Road, Haidian District, Beijing, China
TEL.: +8613391682922; E-MAIL: wangxia2288@sina.com

Submitted: 2025-11-29 Accepted: 2025-12-29 Published online: 2025-12-30

Key words: **Maturity-onset diabetes of the young; hepatocyte nuclear factor 4α; pathogenicity prediction; homology modeling**

Neuroendocrinol Lett 2025; **46**(7):402–409 **PMID:** 41565581 460706 © 2025 Neuroendocrinology Letters • **www.nel.edu**

Abstract

BACKGROUND: This article aims to examine the clinical and familial characteristics of HNF4α-MODY pa-tients who presented with diabetic ketoacidosis (DKA) or diabetic ketosis (DK). Furthermore, it seeks to explore potential pathogenic mechanisms of the HNF4α mutation and to enhance understanding of ketosis susceptibility in this population.

METHODS: We collected detailed medical histories and family histories of two diabetes patients. Whole-exome high-throughput sequencing was performed to identify potential genetic muta-tions. The pathogenicity of the mutations was predicted with PolyPhen-2 and Mutation Taster software. PyMOL software was utilized to analyze the impact of the mutations on the protein structure of HNF4α.

RESULTS: Both probands exhibited a decline in pancreatic islet function following disease onset, leading to ineffective sulfonylurea treatment and the development of DKA or DK. Whole-exome se-quencing revealed distinct heterozygous HNF4α mutations in each family. Proband 1, along with her father and elder daughter, carry the c.1331C>T (p. P444L) mutation. Proband 2 and her father harbored the c.929G>C (p. G310A) mutation. Protein structure predictions indi-cates that the c.1331C>T (p. P444L) mutation induces structural changes in the HNF4α pro-tein. Additionally, the c.929G>C (p. G310A) mutation is identified to disrupt hydrogen bonding interactions between the amino acid at position 310 and its surrounding residues.

CONCLUSION: The G310A variant likely disrupts homodimer stability, impairing islet function, similar to neighboring pathogenic mutations. On the other hand, the P444L variant is considered likely pathogenic, with its variable expressivity within the family being characteristic of MODY. This study demonstrates that some HNF4α-MODY patients may present with DKA or DK, highlighting the condition's clinical heterogeneity.

INTRODUCTION

Maturity-onset diabetes of the young (MODY) is a type of monogenic diabetes that typically manifests in adolescence or young adulthood. It is most commonly inherited in an autosomal dominant manner. Among the 14 identified MODY types (Hattersley *et al.* 2018), HNF4α-MODY, resulting from mutations in the hepatocyte nuclear factor 4α (HNF4α) gene, constitutes a subtype and comprises roughly 14% of all MODY cases (Colclough & Patel, 2022). HNF4α, a member of the nuclear receptor superfamily, is predominantly expressed in the pancreas, liver, intestines, and kidneys. Heterozygous mutations in HNF4α have been implicated in pancreatic β-cell dysfunction, characterized by increased LDL-C levels and de-creased HDL-C and TG levels (Zhang *et al.* 2021). The gene encodes five functional do-mains (A/B to F): an N-terminal activation function domain (AF-1) also known as the A/B domain, two zinc finger C domains responsible for DNA binding (DBD), a potential lig-and-binding domain (LBD) designated D/E, and an HNF-1α transcriptional activation nega-tive regulatory region (F domain) (Beinsteiner *et al.* 2023).

The diagnosis of MODY is established based on the following criteria: onset before 25 years of age, absence of insulin resistance, a family history of diabetes extending over three or more generations, and no need for insulin therapy for a minimum of two years after diagnosis without a propensity for ketoacidosis, Additionally, individuals with MODY typically lack the autoantibodies associated with type 1 diabetes mellitus (T1DM) (Urakami, 2019). However, previously reported cases indicate that the absence of these features, such as a family history of diabetes, age of onset exceeding 25 years, or presence of ketosis tendency, does not necessarily exclude MODY (Karaoglan & Nacarkahya, 2021). Although HNF4α-MODY is increasingly identified, cases presenting with DKA are exceptionally rare. This study aimed to summarize the clinical features and family characteristics of two patients with HNF4α-MODY and DKA or DK. To explore the HNF4α mutation gene spectrum and raise awareness of the ketosis susceptibility in HNF4α-MODY patients, we analyzed the structure and pathogenic mechanisms of HNF4α mutation sites through predictive analysis.

METHODS

Study object

This study was reviewed and approved by the Ethics Committee of the First Medical Center, Chinese PLA General Hospital. All study subjects signed the consent form, and for non-adult subjects, consent was obtained from their supervisors.

Proband 1

Proband 1 was a 32-year-old married woman who presented with hyperglycemia during her pregnancy in 2022. At 8 weeks of gestation, elevated fasting plasma glucose (FPG) levels were detected, ranging from 7.0 to 8.0 mmol/L. Despite the absence of typical diabetic symptoms, she was diagnosed with gestational diabetes mellitus and detemir insulin therapy was initiated resulting in good glycemic control. However, at the 15th week of gestation she presented polydipsia, polyuria, and fatigue. Investigations revealed a random blood glucose level of 23.29 mmol/L, strongly positive urine ketones (+++). Following an induced abortion due to fetal demise, her treatment regimen was adjusted to aspart and detemir insulin injection. However, this regimen proved ineffective due to persistent blood glucose fluctuations and recurrent episodes of pre-meal hypoglycemia. Therefore, in February 2023, her treatment regimen was further modified to subcutaneous insulin aspart (26.4 units/day) in combination with metformin (1.0 g once nightly).

Proband 1 gave birth to two daughters in 2015 and 2019, respectively, with birth weights of 4.0 kg and 3.6 kg. Both deliveries were vaginal and without complications. Notably, there was no family history of diabetes in her parents or other known relatives.

Proband 2

Proband 2 was a 34-year-old married woman diagnosed with type 2 diabetes mellitus (T2DM) in a routine health check-up six years before. At the time of diagnosis, her FPG level was 10.0 mmol/L, but she did not present any classical symptoms of diabetes such as polydipsia, polyuria, polyphagia, or weight loss. Initially, she was treated with a combination of glargine insulin and acarbose, achieving good glycemic control within six months. However, the hyperglycemia persisted, and her treatment regimen was switched back to glargine insulin and acarbose. Despite this adjustment, follow up assessments revealed poor glycemic control, with an HbA1c of 11%, FPG of 13.18 mmol/L, and the presence of urine ketones.

The father of proband 2 was diagnosed with T2DM at the age of 45 and currently maintains good glycemic control with a regimen of sitagliptin (5 mg once daily) and metformin (0.5 g at lunch and before dinner). The mother of proband 2 was diagnosed with T2DM at the age of 60 and also maintains good glycemic control with a regimen of glimepiride (1 mg once daily) and metformin (0.5 g at lunch and before dinner). Additionally, both her paternal and grandfathers were diagnosed with T2DM after middle age.

Clinical data collection

Detailed medical histories were collected from the proband and their family members. Height and weight measurements were taken, and body mass index (BMI) was calculated. Clinical and biochemical data were collected for all family members. Anti-glutamic acid decarboxylase antibodies (GAD), anti-islet cell antibodies (IAA), zinc transporter 8 antibodies (ZnT8),

Tab. 1. Clinical Features and biochemical data of Family Members with HNF4α-MODY

Member Phenotype	Family Pedigree 1					Family Pedigree 2		
	Proband 1	Proband 1's father	Proband 1's mother	Proband 1's elder daughter	Proband 1's younger daughter	Proband 2	Proband 2's father	Proband 2's mother
Age (years)	32	58	59	9	5	34	63	62
Age at onset of diabetes (years)	31	NF	NF	NF	NF	28	45	60
Duration of diabetes (years)	1	NA	NA	NA	NA	6	18	1
BMI (kg/m^2)	23.0	NA	NA	NA	NA	21.5	NA	NA
HbA_{1c}(%)	NA	4.9	5.0	NA	NA	NA	NA	NA
FPG (mmol/L)	7.16	5.52	5.5	5.24	4.87	8.53	NA	NA
1hPG (mmol/L)	17.55	11.3	6.7	NA	NA	NA	NA	NA
2hPG (mmol/L)	24.83	10.49	6.31	5.29	5.11	27.24	NA	NA
Fasting C-peptide (ng/ml)	0.06	2.26	4.16	1.21	0.73	1.61	NA	NA
1h C-peptide (ng/ml)	0.12	7.06	8.45	NA	NA	NA	NA	NA
2h C-peptide (ng/ml)	0.19	10.6	4.05	1.54	1.88	3.96	NA	NA
FINS (mU/L)	0.2	5.14	31.45	7.11	4.0	4.09	NA	NA
1h-INS (mU/L)	0.2	51.55	85.91	NA	NA	NA	NA	NA
2h-INS (mU/L)	0.2	45.11	11.32	8.51	8.6	25.667	NA	NA

Note:HbA1c (%) reference range: 3.8%-5.8%; FPG (fasting plasma glucose) reference range: 3.89-6.11 mmol/L; 2hPG (2-hour postprandial glucose) reference range: ≤7.8 mmol/L; Fasting C-peptide reference range: 1.1-4.4 ng/ml; Ins (insulin release test); FINS, fasting insulin : reference range 2.56-24.84 mU/L;1h-INS, 1-hour insulin;2h-INS, 2-hour insulin;NA: not applicable;NF: not found

protein tyrosine phosphatase antibodies (IA-2A), and insulin autoantibodies were measured by enzyme-linked immunosorbent assay (ELISA).Anti-islet cell antibodies (ICA) were measured by indirect immunofluorescence assay.

Whole-exome sequencing

The QIAamp DNA extraction kit (QIAGEN, Germany) was used to extract genomic DNA from the peripheral blood of proband 1, 2 and their family members. This extracted DNA was then fragmented and libraries were constructed, followed by target enrichment of DNA from the desired gene exons and adjacent splice sites using the Roche KAPA Hyper Exome kit, and subsequently sequenced on the MGISEQ-2000 platform to identify genetic variants. The sequencing reads were aligned against the UCSC hg19 human reference genome utilizing the Burrows-Wheeler Aligner (BWA) tool, with subsequent removal of duplicate reads. Var-iant calling, including single nucleotide variants (SNVs), insertions/deletions (INDELs), and genotype assignment, was conducted using the Genome Analysis Toolkit (GATK) available at https://software.broadinstitute.org/gatk/. Detection of copy number variations at the exome level was carried out using the Exome Depth tool.

Pathogenicity prediction analysis

The pathogenicity of the identified mutations was predicted using online tools PolyPhen-2 (http://genetics.bwh.harvard.edu/pph2/) and Mutation Taster (https://www.genecascade.org/MutationTaster2-021/#transcript) (Steinhaus *et al.* 2021). These tools were applied to the mutations defected in proband 1 and proband 2, respectively. To further assess the clinical significance of these variants, they were classified into five cat-egories according to the American College of Medical Genetics and Genomics (ACMG) guidelines for interpreting sequence variations: "pathogenic," "likely pathogenic," "uncertain significance," "likely benign," and "benign" (Fatkin & Johnson, 2020).

Analysis of the conservation of mutation sites

To assess the evolutionary conservation of the identified mutations, the HNF4α encoded amino acid sequences from seven vertebrate species were analyzed.

MEGA software was used to align the sequences from human (NM_175914.5), pig (NM_001044571.1), Norwe-gian rabbit (NM_001270931.1), house mouse (NM_001312906.1), rhesus monkey (XM_015148955.2), zebrafish (NM_194368.1), and cattle (NM_001015557.1). These gene sequences were obtained from the NCBI GenBank database. Next, the impact of the muta-tions on protein structure was investigated. PSIPRED Workbench (http://bioinf.cs.ucl.ac.uk/psipred/) was used to predict the secondary structures of both wild-type HNF4α (NM_175914.4) and the mutated protein. Additionally, the AlphaFold2 online server (https://colab.research.google.com/github/sokrypton/ColabFold/blob/main/AlphaFold2.ipynb) was utilized to build three-dimensional models of both wild-type and mutated HNF4α. Final-ly, PyMOL software was employed to analyze and compare the tertiary structures of the pro-teins.

RESULTS

Clinical course and laboratory investigations

The clinical characteristics of the two families were summarized in Table 1. Several autoantibodies associated with T1DM, including (GAD), (ICA), (IAA), (ZnT8), (IA-2A) were all negative in proband 1 and proband 2.

Proband 1 presented with hyperglycemia and DKA during the third pregnancy. Subsequent tests revealed low basal levels of C-peptide and insulin, indicating impaired islet function. At the time of admission, Proband 1 presented with an HbA1c of 8.8% and FPG of 14.8 mmol/L. Other laboratory tests, including liver and kidney function, were normal. Physical examination revealed no abnormalities detected in heart, lung, and abdominal examinations. Because the observed decline in islet function and the risk of rapid deterioration, insulin pump therapy with insulin aspart was initiated after admission and continued for management. To further optimize glycemic control, an attempt was performed to add glimepiride while maintaining the current insulin regimen. Five days post-glimepiride initiation, her fasting and 2-hour postprandial blood glucose levels were 6.66 and 16.27 mmol/L, respectively, with C-peptide levels of 0.06 and 0.15 ng/ml, and insulin levels of 0.20 and <0.20 mU/L, respectively. Both pre- and postprandial C-peptide and insulin levels were low with no significant peak observed. This indicated persistent impaired islet function and inadequate glycemic control despite the addition of sulfonylurea therapy.

It is noteworthy that the father of proband 1 was found to have a 1-hour postprandial glucose (1hPG) of 11.3 mmol/L and a 2-hour postprandial glucose (2hPG) of 10.49 mmol/L in this examination, meeting the clinical diagnostic criteria for impaired glucose tolerance (IGT).

On admission, laboratory tests for Proband 2 revealed ketonuria (KET +) and markedly elevated blood glucose (+++). Arterial blood gas analysis ruled out acidosis.Physical examination showed of the heart, lungs, and abdomen were normal. Proband 2's plasma glucose was poorly controlled with oral hypoglycemic medications, and laboratory tests revealed insufficient pancreatic islet function with a propensity for ketosis. Given these findings, the treatment plan was modified to involve subcutaneous injections aspart and detemir insulin, and got to effective blood sugar control.

Results of whole-exome sequencing

Whole-exome sequencing revealed a heterozygous HNF4α (chr20:43058277) NM_175914.4: c.1331C>T (p.Pro444Leu) mutation in proband 1(Figure 1A). This mutation was also id-entified in her father an delder daughter, but was absent in proband 1's mother and younger daughter (Figure 1B). Whole-exome sequencing revealed that proband 2 and her father both carried a heterozygous HNF4α mutation (chr2-0:43052760) NM_175914.4: c.929G>C (p.Gly310Ala) (Figure 1C). However, this mutation was not det-ected in her mother (Figure 1D).

Pathogenicity prediction of the mutation sites

Alignment of HNF4α amino acid sequences from seven vertebrate species using MEGA software revealed that both mutation sites are highly conserved across different species. However, computational predictions yielded discordant results. Although Proband 1 presented with DKA, PolyPhen-2 and Mutation Taster software predicted the HNF4α c.1331C>T (p. Pro444Leu) mutation carried by proband 1 to be benign (PolyPhen-2 score: 0.001), suggesting algorithmic limitations. In contrast, HNF4α c.929G>C (p. Gly310Ala) mutation carried by Proband 2 was consistently predicted to be pathogenic (PolyPhen-2 score: 1.000; Mutation Taster prediction: "Deleterious").

A systematic application of the ACMG guidelines to the available evidence classifies P444L as a Variant of Uncertain Significance (VUS) due to the conflict between in silico predictions and the observed severe phenotype, whereas G310A meets the criteria for a Likely Pathogenic variant. This comparison underscores that in silico prediction tools cannot substitute for functional validation in clinical diagnosis.

Analysis of predicted protein structure

PSIPRED Workbench was used to predict the secondary structures of wild-type HNF4α, HNF4α p. P444L, and HNF4α p. G310A proteins. The results showed that while both mutation sites (310 and 444) are located in flexible, unstructured loops rather than rigid helices, these mutations still altered the stability of adjacent α-helix and β-sheet regions of the HNF4α protein. The HNF4α structural domains containing the two mutation sites are shown in Figure 2.

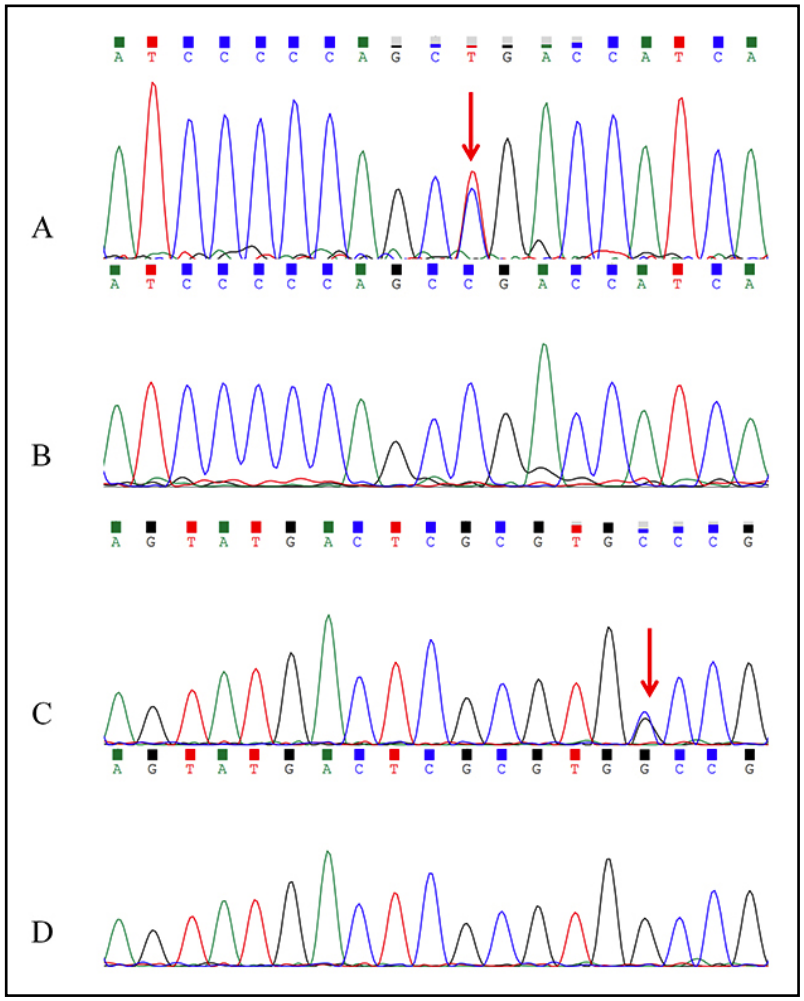

Fig. 1. Sequencing chromatograms of HNF4α gene in family pedigree 1 and family pedigree 2
(A) Sequencing chromatograms of proband 1, her father, and eldest daughter. The arrow in-dicates the heterozygous mutation HNF4α(chr20:4305 8277)NM_175914.4: c.1331C>T(p.Pro444Leu) carried by all three individuals. **(B)** Sequencing chromatograms of proband 1's mother and second daughter, showing that they do not carry the mutation. **(C)** Sequencing chromatograms of proband 2 and her father. The arrow indicates the heterozy-gous mutation HNF4α (chr20:4305 8277) NM_175914.4: c.929G>C(p.Gly310Ala) carried by both individuals. **(D)** Sequencing chromatogram of proband 2's mother, showing that she does not carry the mutation.

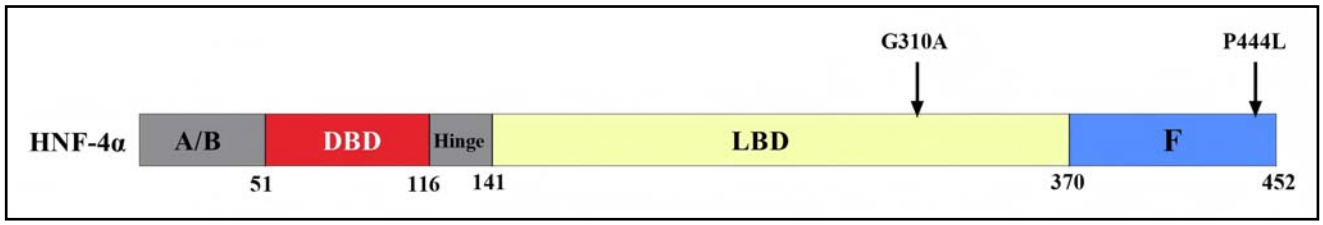

Fig. 2. HNF4α protein structural domains containing the G310A and P444L mutation sites.

Analysis of the protein tertiary structures using PyMOL software revealed that the P444L mutation alters the three-dimensional structure of the protein. Similarly, the G310A mutation, which changes a glycine to an alanine, also impacts the protein structure. Before the mutation, G310 forms hydrogen bonds with G313 and E314. After the mutation, glycine is replaced by alanine, resulting in the loss of the hydrogen bond with G313 and the formation of a new hydrogen bond with S308. This change in hydrogen bonding ultimately leads to a modified protein structure of HNF4α (Figure 3).

DISCUSSIONS

We reported two families carrying different heterozygous HNF4α gene mutations, highlighting the variable phenotypes observed even among probands and their family members carrying the same mutation. In the HNF4α p. P444L mutant carried by proband 1, the 444th amino acid changes from a nonpolar hydrophobic proline to a nonpolar hydrophobic leucine, a substitution with minimal physicochemical difference. The mutation site c.1331C>T is located in exon 9, within the F functional domain of the protein. This region is critical for activating gene expression by HNF4α. Previously, a missense mutation in the F domain, HNF4α p.V393I, was identified in a French family with diabetes diagnosed at age 45. This mutation was associated with a significant reduction in transcriptional capacity, leading to impaired insulin secretion (Amara *et al.* 2015). However, it is important to note that some non-diabetic probands between 30 and 40 years old were also carriers of HNF4α p.V393I (Hani *et al.* 1998) .

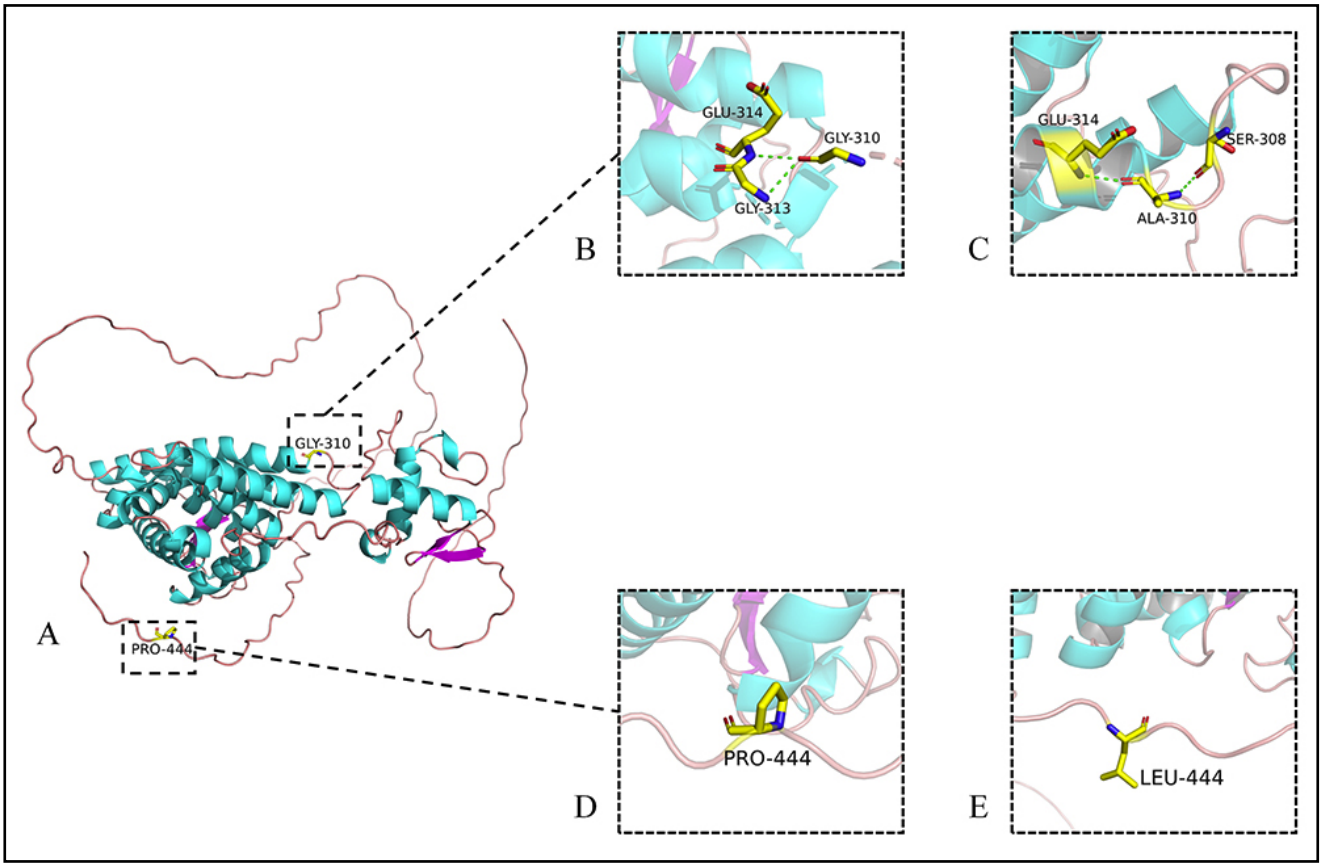

Fig. 3. Predicted structural impact of P444L and G310A mutations on HNF4α.
Structures were modeled using AlphaFold2 and analyzed in PyMOL.
(A) Full-length HNF4α showing mutation sites (red spheres) relative to functional domains: DNA-binding (blue), Hinge (green), Ligand-binding (LBD, yellow), and F-domain (red).
(B-C) P444L Analysis: Comparison of wild-type Pro444 **(B)** and mutant Leu444 **(C)** within the F-domain regulatory region. The P444L substitution replaces a rigid proline with a flexi-ble leucine, predicted to alter local backbone geometry (yellow dashed lines) and potentially disrupt coregulator interactions.
(D-E) G310A Analysis: Hydrogen bonding at the LBD dimerization interface. **(D)** Wild-type Gly310 is stabilized by H-bonds with Gly313 (2.9 Å) and Glu314. **(E)** Mutant Ala310 dis-rupts the G310-G313 bond (distance increased >4 Å) and forms a novel bond with Ser308. This remodeling likely destabilizes the homodimer interface, consistent with its proximity to established pathogenic mutations I314F and R324H.
Note: Hydrogen bond distances are model-derived estimates requiring experimental validation (e.g., X-ray crystallography).

Similarly, in our study, genetic testing revealed that both the father and the elder daughter of proband 1 carry the HNF4α p.P444L variant. However, unlike the case of proband 1, who experienced rapid decline in islet function during pregnancy accompanied by diabetic ketoac-idosis and had a low baseline C-peptide level, the carriers within her family exhibited milder phenotypes. Her father was identified with prediabetes during examination, and her elder daughter did not show typical diabetic symptoms. Both maintained normal islet function.This significant phenotypic discrepancy within the family—with proband 1 showing β-cell failure (fasting C-peptide 0.06 ng/ml) and DKA while her father and daughter retain preserved func-tion (C-peptide 2.26 and 1.21 ng/ml, respectively)—suggests a mechanism involving incomplete penetrance or synergistic stressors (e.g., pregnancy) rather than a simple monogenic effect. This indicates that the P444L variant is likely pathogenic, and its phenotypic variability within the family aligns with the characteristic variable expressivity of MODY.

The HNF4α p. G310A mutation identified in proband 2 involves a substitution of the amino acid glycine at position 310 with alanine. Both glycine and alanine are nonpolar amino acids; however, glycine is weakly hydrophobic, while alanine exhibits stronger hydrophobic prop-erties. It is predicted to enhance the hydrophobic effect, thereby promoting protein folding. However, secondary structure prediction revealed a change in protein structure, with an in-crease in α-helix and random coil regions and a decrease in β-sheet folding after the mutation. PyMOL analysis of the three-dimensional structures of G310 and mutant G310A showed the disappearance of the hydrogen bond between G310 and G313 and the formation of new hy-drogen bonds between G310A and S308 and E314, respectively. The-se changes in interactions with surrounding residues may affect the

function and stability of the HNF4α protein, warranting further experiments for verification. Additionally, the mutation site c.929G>C is located in exon 8, within the ligand-binding domain (LBD) of HNF4α. Studies have shown that HNF4αbinds to DNA as a dimer, with its dimerization interface spanning the LBD. The LBD interacts with ligands (small molecules or other proteins) and coactivators to regulate gene expression. It is speculated that the G310A mutation may affect the HNF4α dimerization interface, as it is located in close proximity to other mutations (I314F and R324H) that have been shown to disrupt dimerization. One study detected that HNF4α mutants I314F and R324H, as well as their neighboring residues (R322A, Q318A, D316A, and N315A), are located in the LBD and at the structural hub where the DNA-binding and ligand-binding domains intersect. These mutations reduce the DNA affinity and transcrip-tional activity of the receptor (Chandra *et al.* 2013). The G310A mutant carried by proband 2 is also located in the LBD at this critical domain junction. G310A disrupts the G310-G313 hydrogen bond at the dimerization interface, a region located proximally to validated pathogenic mutations I314F and R324H. Given its position within this critical structural domain and Proband 2's clinical presentation of insulin dependence (C-peptide 1.61 ng/ml), it is plausible that the G310A variant impairs HNF4α function by destabilizing the homodimer, thereby reducing its DNA-binding affinity and transcriptional activity—a mechanism poten-tially analogous to its neighboring pathogenic variants. However, confirming this specific mechanistic pathway requires direct biochemical validation, for example, by electrophoretic mobility shift assay (EMSA) or co-immunoprecipitation (Co-IP) beyond computational structural modeling.

The clinical phenotype of HNF4α-MODY varies among patients with different mutations and even within family members carrying the same mutation. This variability may be due to fac-tors such as genetic background, environmental influences, and epigenetic modifications. Younger generations in multigenerational families often exhibit earlier onset age and more severe phenotypes (Zhang *et al.* 2023). Similar findings have been observed in studies of other MODY subtypes. For example, phenotypic variabilities including age at diagnosis, treatment requirements, and complications, have been observed in the same family members and among families with the same HNF1α mutation, suggesting that environmental influences such as obesity or the intrauterine environment, genetic modifiers may all have impacts on the phenotype (Li *et al.* 2022). Proband 1 experienced rapid islet function decline during preg-nancy and developed DKA quickly. Oral glucose tolerance test indicated low basal C-peptide and insulin levels, suggesting poor islet function. In contrast, while proband 1`s father and elder daughter both carry the same variant, they exhibit milder phenotypes. The father pre-sented with asymptomatic impaired glucose tolerance (IGT), and the elder daughter showed no diabetic symptoms; both maintained normal islet function based on oral glucose tolerance tests. Proband 2 had poor glycemic control with oral medications and required insulin therapy, while her father achieves well glycemic control with two oral antidiabetic medicine. The con-trasting clinical presentations of probands 1 and 2, as well as the observed variability within their families, highlight the significant clinical heterogeneity in HNF4α-MODY patients.

In conclusion, this study characterized two HNF4α gene variants, P444L and G310A, identified in two distinct families. Structural and phenotypic analyses suggest that the G310A variant likely disrupts homodimer stability, thereby impairing islet function—a mechanism analogous to neighboring pathogenic mutations, though further validation by biochemical assays such as EMSA or Co-IP is warranted. Meanwhile, the phenotypic variability observed in the family carrying the P444L variant corresponds to the variable expressivity typical of MODY, supporting its classification as likely pathogenic. Clinically, HNF4α-MODY may manifest as diabetes mellitus, with severe presentations including diabetic DK or DKA, highlighting its broad phenotypic spectrum. These findings offer relevant insights for the clinical differentiation and diagnosis of this condition.

AUTHOR CONTRIBUTIONS

Jie Lu and Xianling Wang conceived and designed the study. Jilai Zhang was involved in the acquisition of data. Jie Lu drafted the manuscript. Xianling Wang contributed to the critical revision of the manuscript for important intellectual content. All authors approved the final manuscript for publication. Xianling Wang is the guarantor, maintaining full access to all the data in the study and taking responsibility for the integ rity of the data and the accuracy of the analysis.

ACKNOWLEDGEMENTS

We thank the probands and their families for supporting and participating in this study.

FUNDING INFORMATION

This study did not receive any specific grant from funding agencies in the public, commercial, or not-for-profit sectors.

CONFLICT OF INTEREST STATEMENT

The authors declare that they have no conflicts of interest.

REFERENCES

1 Amara A, Ben Charfeddine I, Ghédir H, Othman HB, Béji C, Achour A et al. (2015). Frequency of hnf4a-p.i463v variant in the tunisian north-african population and its relation with diabetes mellitus. Iran J Public Health. **44**(3): 396–403.

2 Beinsteiner B, Billas IML, Moras D (2023). Structural insights into the hnf4 biology. Front Endocrinol (Lausanne). **14**: 1197063. doi:10.3389/fendo.2023.1197063.

3 Chandra V, Huang P, Potluri N, Wu D, Kim Y, Rastinejad F (2013). Multidomain integration in the structure of the HNF4α nuclear receptor complex. Nature. **495**(7441): 394–398. doi:10.1038/nature11966.

4 Colclough K, Patel K (2022). How do i diagnose maturity onset diabetes of the young in my patients? Clin Endocrinol (Oxf). **97**(4): 436–447. doi:10.1111/cen.14744.

5 Fatkin D, Johnson R (2020). Variants of uncertain significance and "missing pathogenicity". J Am Heart Assoc. **9**(3): e015588. doi:10.1161/JAHA.119.015588.

6 Hani EH, Suaud L, Boutin P, Chèvre JC, Durand E, Philippi A et al. (1998). A missense mutation in hepatocyte nuclear factor-4 alpha, resulting in a reduced transactivation activity, in human late-onset non-insulin-dependent diabetes mellitus. J Clin Invest. **101**(3): 521–526. doi:10.1172/JCI1403.

7 Hattersley AT, Greeley SAW, Polak M, Rubio-Cabezas O, Njølstad PR, Mlynarski W (2018). ISPAD clinical practice consensus guidelines 2018: the diagnosis and management of monogenic diabetes in children and adolescents. Pediatr Diabetes. **19**(S27): 47–63. doi:10.1111/pedi.12772.

8 Karaoglan M, Nacarkahya G (2021). Clinical and laboratory clues of maturity-onset diabetes of the young and determination of association with molecular diagnosis. J Diabetes. **13**(2): 154–163. doi:10.1111/1753-0407.13097.

9 Li LM, Jiang BG, Sun LL (2022). HNF1A: From monogenic diabetes to type 2 diabetes and gestational diabetes mellitus. Front Endocrinol (Lausanne). **13**: 829565. doi:10.3389/fendo.2022.829565.

10 Steinhaus R, Proft S, Schuelke M, Cooper DN, Schwarz JM, Seelow D (2021). MutationTaster2021. Nucleic Acids Res. **49**(W1): W446–W451. doi:10.1093/nar/gkab266.

11 Urakami T (2019). Maturity-onset diabetes of the young (mody): current perspectives on diagnosis and treatment. Diabetes Metab Syndr Obes. **12**: 1047–1056. doi:10.2147/DMSO.S179793.

12 Zhang H, Colclough K, Gloyn AL, Pollin TI (2021). Monogenic diabetes: a gateway to precision medicine in diabetes. J Clin Invest. **131**(3): e142244. doi:10.1172/JCI142244.

13 Zhang J, Jiang Y, Li J, Li L, Chen S, Hong J et al. (2023). Identification and precision therapy for three maturity-onset diabetes of the young (mody) families caused by mutations in the hnf4a gene. Front Endocrinol (Lausanne). **14**: 1237553. doi:10.3389/fendo.2023.1237553.